

# Microstructure of a nickel insert, a special copper alloy, and a cast joint between them

## Mikrostruktura nikljevega vstavka, posebne bakrove zlitine in litega spoja med njima

Iztok Naglič<sup>1,\*</sup>, Žan Kresnik<sup>2</sup>, Andrej Resnik<sup>2</sup>, Boštjan Markoli<sup>1</sup>

<sup>1</sup>University of Ljubljana, Faculty of Natural Sciences and Engineering, Aškerčeva cesta 12, 1000 Ljubljana, Slovenia

<sup>2</sup>OMCO Metals Slovenia d.o.o., Cesta Žalskega tabora 10, 3310 Žalec, Slovenia

\*Corresponding author: E-mail: iztok.naglic@ntf.uni-lj.si

### Abstract in English

This work deals with the characterisation of the microstructure of a nickel insert, a special copper alloy and the cast joint between them after their use as a glass manufacturing mould. The microstructure was characterised by optical microscopy, scanning electron microscopy and microanalysis by energy dispersive X-ray spectroscopy.

It was found that the nickel insert contained 7 at. % Si and 0.3 at. % Fe. The special copper alloy contains undesirable phases or compounds, including lead, aluminium-based oxides and borides. The borides are either iron-, iron-chromium- or chromium-based with different stoichiometries between metal components and boron. The cast joint between the nickel insert and the special copper alloy has evidence of mixing the two alloys, while only in some areas porosity and oxides prevented the formation of a suitable cast joint. Aluminium-based oxides and some borides could be the cause of the formation of cracks due to their morphology.

**Keywords:** nickel alloy, copper alloy, microstructure, microanalysis

### Introduction

Moulds for glass production are usually made of special copper alloys. Standardised copper alloys for these purposes are designated as C99300 and C99350 according to UNS [1–3]. In addition to copper, these alloys usually contain some nickel, aluminium, zinc, and iron as the main alloying elements and should have high hardness, oxidation resistance, and resistance

### Povzetek

Delo obravnava karakterizacijo mikrostrukture nikljevega vstavka, posebne bakrove zlitine in litega spoja med njima po uporabi kot kalupa za oblikovanje stekla. Mikrostrukturo smo karakterizirali z optično mikroskopijo, vrstično elektronsko mikroskopijo in mikroanalizo z energijsko disperzijsko rentgensko spektroskopijo.

Ugotovljeno je bilo, da nikljev vstavek vsebuje 7 at. % silicija in 0,3 at. % železa. Posebna bakrova zlitina vsebuje nezaželene faze, kot so svinec, oksidi na osnovi aluminija in boridi. Boridi so železovi, železo-kromovi ali le kromovi z različnimi stehiometrijami med kovinami in borom. Na litem spoju med nikljevim vstavkom in posebno bakrovo zlitino je opazno mešanje obeh zlitin, le na nekaterih mestih pa so poroznost in oksidi preprečili nastanek ustreznega litega spoja. Oksidi na osnovi aluminija in nekateri boridi lahko zaradi svoje morfologije povzročijo nastanek razpok.

**Ključne besede:** nikljeva zlitina, bakrova zlitina, mikrostruktura, mikroanaliza

to thermal fatigue. In the glass mould industry, a slightly modified special copper alloy is often used, which in addition to copper also contains 15–16.5 wt. % Ni, 9.5–10.0 wt. % Al, 7.5–9.0 wt. % Zn, 0.8–1.2 wt. % Si and up to 1.25 wt. % Fe, 0.2 wt. % Mn, 0.15 wt. % P, 0.1 wt. % Sn, 0.1 wt. % Pb, 0.1 wt. % Cr, 0.1 wt. % Mg and 0.1 wt. % Sb. The microstructure of these alloys generally consists of face-centred cubic  $\alpha_{Cu}$  and cubic  $\beta$ -AlNi intermetallic phases or compounds with

space group Pm-3m (CsCl prototype) [4, 5]. A considerable amount of copper is soluble in the intermetallic  $\beta$ -AlNi phase, which affects its lattice parameters and mechanical properties [6].

The moulds for making glass have nickel inserts and nickel plates in certain places. The nickel inserts have a cast joint with a special copper alloy, while the nickel plates are welded to a special copper alloy using a boron-containing additive. This boron can form very stable borides with iron and chromium [7-9]. The moulds for glass production are recycled together with the nickel inserts and plates after their end-of-life cycle. The amount of recycled material in the production of a new special copper alloy is limited because of the need to obtain the correct chemical composition of the alloy and to limit other undesirable compounds that accumulate in the alloy.

The objective of this work was to characterise the composition and microstructure of the nickel insert, the special copper alloy, and the cast joint after their end-of-life cycle as a glass manufacturing mould.

## Materials and methods

This paper characterises the microstructure of the cast joint between a nickel insert and a special copper alloy, which is part of a mould used for the production of glass products. The special copper alloy presented in this work was made from used casting moulds. This mould was analysed after the end of its life cycle. The joint between a nickel insert and a special copper alloy was cut out of the used mould. Smaller pieces were mounted and metallographically prepared for light and scanning electron microscopy by grinding and polishing with diamond paste. Final polishing was performed with a  $\text{SiO}_2$  suspension.

Characterisation of the microstructure of the nickel insert, the special copper alloy and its cast joint was performed using optical microscopy, scanning electron microscopy (SEM), and microanalysis. Light microscopy was performed using a Zeiss Axio Imager A1m with AxioCam ICc 3 and AxioVision software, while SEM and microanalysis were performed using a JEOL JSM-7600F scanning electron microscope

with field emission gun and energy dispersive X-ray spectroscopy (EDS) at an accelerating voltage of 20 kV.

## Results and discussion

The average chemical composition, determined by EDS, is shown in Table 1. The results show that the nickel insert consists of silicon and iron in addition to nickel. The microstructure of a nickel insert is shown in Figure 1. The light microscopy image of the microstructure in Figure 1a shows that large nickel dendrites are present. The backscattered electron image (BE) of the interdendritic region is shown in Figure 1b. This region consists of a heterogeneous structure of nickel and one or more intermetallic phases, which could be either  $\beta_3$ -Ni<sub>3</sub>Si,  $\beta_2$ -Ni<sub>3</sub>Si,  $\gamma$ -Ni<sub>31</sub>Si<sub>12</sub> or  $\beta_1$ -Ni<sub>3</sub>Si according to the binary Ni-Si system [10-12]. According to this system, 3.5 wt. % Si lowers the liquidus and solidus to about 1380 and 1310 °C, respectively.

Figure 2 shows the microstructure of the special copper alloy. The chemical composition of this alloy, determined by EDS, is given in Table 2. Among the elements found in the alloy, the most important is iron, whose content is limited in these alloys. Solidification of such an alloy begins with primary solidification of the intermetallic  $\beta$ -AlNi phase, followed by a eutectic reaction forming a heterogeneous structure of  $\alpha_{\text{Cu}}$  and  $\beta$ -AlNi [13]. Upon further cooling, the solubility of copper in the  $\beta$ -AlNi phase decreases, and  $\alpha_{\text{Cu}}$  precipitates within the intermetallic  $\beta$ -AlNi phase [13]. In addition to these two phases, other phases are present as inclusions in the microstructure. These phases are present due to recycling. As shown in Figure 2c, these phases are darker than  $\alpha_{\text{Cu}}$  and the intermetallic  $\beta$ -AlNi phase. This fact indicates that these regions consist of a significant amount of elements with low atomic number.

**Table 1:** Chemical composition of the nickel insert determined by EDS.

	Ni	Si	Fe
at. %	92.8	7	0.3
wt. %	96.3	3.5	0.3

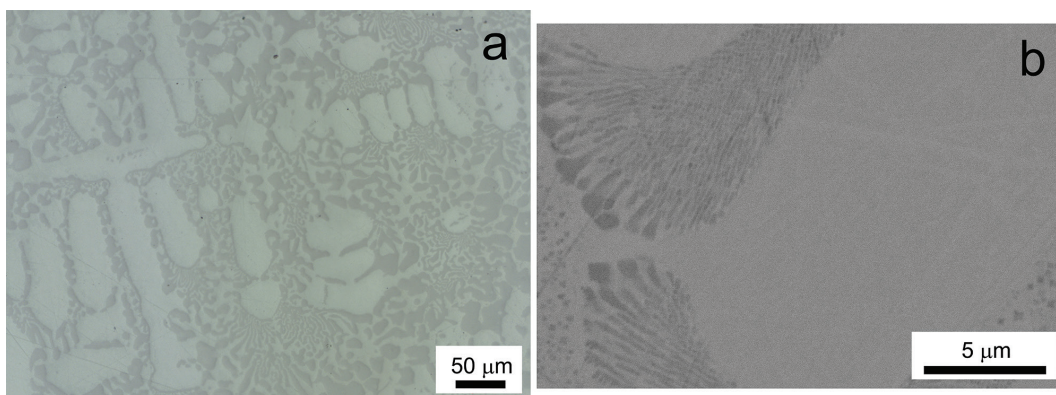


**Figure 1:** Light microscopy image (a) and BE image (b) of the nickel insert.

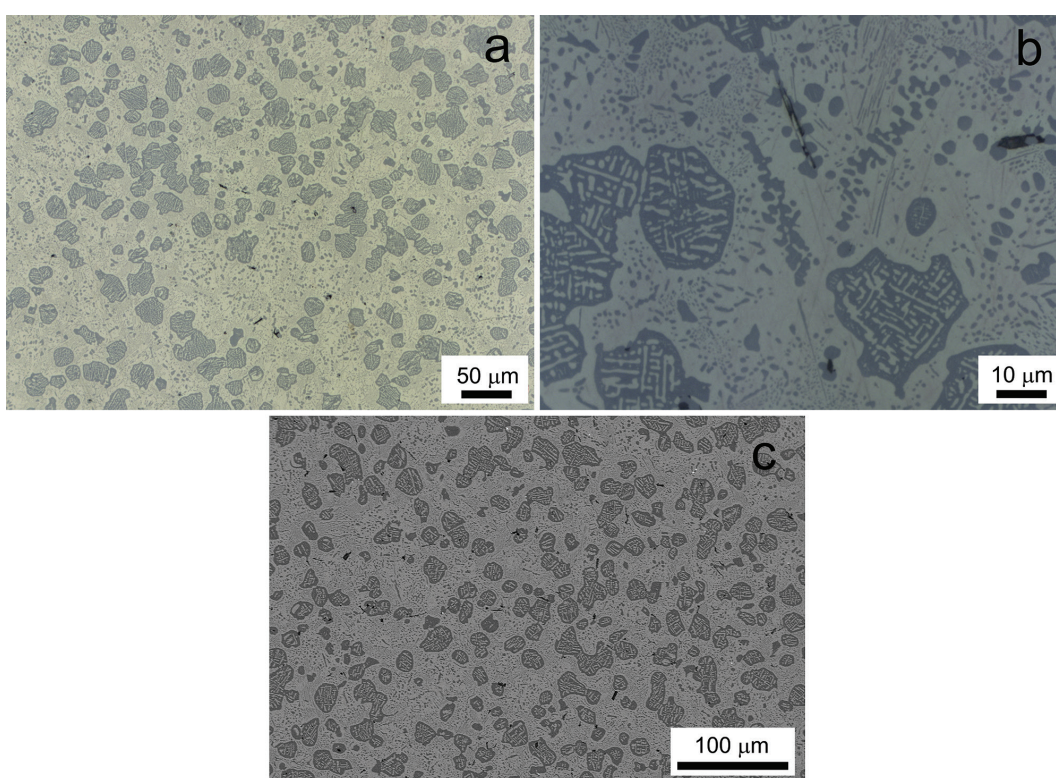


**Figure 2:** Light (a, b) and BE (c) images of the microstructure of a special copper alloy.

**Table 2:** Chemical composition of the special copper alloy determined by EDS.

	Cu	Ni	Al	Zn	Si	Fe
at. %	52.6	16.6	21.5	5.9	2.4	1.0
wt. %	61.8	18.0	10.7	7.1	1.2	1.0

Figure 3 shows a higher magnification BE image with marked areas of microanalyses of the special copper alloy containing several darker and lighter phases. The results of the

microanalyses are shown in Table 3. The areas labelled 1 and 2 represent lead, which is very bright on the BE image due to its high atomic number. The regions labelled 3 and 4 are

related to darker phases on the BE image and consist predominantly of boron. Region 3 contains mostly chromium, but also some iron and manganese. Other elements, including copper and nickel, are detected due to the low analytical spatial resolution. Considering only boron, chromium, iron, and manganese, this boride has a composition of 78.9 at. % B, 17.2 at. % Cr, 3.6 at. % Fe, and 0.3 at. % Mn. According to the binary B-Cr and B-Fe and ternary B-Cr-Fe and B-Fe-Mn systems [7–9, 14], this boride could be of the  $\text{CrB}_4$  type with the space group Immm. This boride can contain up to 7 at. % Fe at an equilibrium temperature of 1080 °C [9].

The boride in Region 4 contains predominantly chromium, iron and manganese, while other elements with significant contents were detected due to low analytical spatial resolution. Considering only these four elements, the composition of this boride is 67.5 at. % B, 16.1 at. % Cr, 15.5 at. % Fe and 0.9 at. % Mn. The composition of this boride is very close to the  $\text{CrB}_2$  boride type with space group P6/mmm [7, 9]. According to the ternary B-Cr-Fe system

[9], this boride can only contain up to 2 at. % Fe at 1080 °C. However, the temperature commonly used in melting and holding the melt of this particular copper alloy is much higher. The liquidus temperature for the copper alloy in question was found to be between 1170 and 1180 °C [13], while the melt is normally held at temperatures at least 100 °C higher during the production process. This means that the borides are kept at temperatures probably at least 200 °C higher than the temperature designated in the ternary B-Cr-Fe system [9]. This could also mean that the solubility of the iron could be higher at these temperatures. Lastly, it is possible that the boride itself is not an equilibrium phase at all. The solubility of the 0.9 at. % Mn is quite likely; however, since manganese itself forms  $\text{MnB}_2$  with the same crystal structure and space group P6/mmm, it is hard to tell them apart [14, 15]. Yet, the boride in Region 4 exhibits an acicular morphology, which is a typical characteristic of hexagonal phases or compounds.

Region 5 corresponds to a copper-rich cubic solid solution that also contains aluminium, zinc and some nickel. Region 6 is related to the  $\beta\text{-AlNi}$  intermetallic phase that contains aluminium and nickel as well as copper, silicon and some iron. The detection of zinc in Region 6 is most likely again the result of low analytical spatial resolution.

Figure 4 shows the BE image of the special copper alloy at various magnifications. Figure 4b also shows the regions of the microanalyses, which correspond to a darker particle similar to the borides in Figure 3 in the first case and a large dark and thin phase in the second and third. The results of the microanalyses are shown in Table 4.

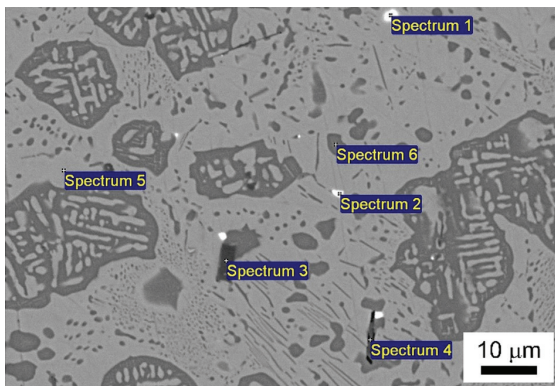


**Figure 3:** BE Image of the microstructure of a special copper alloy with marked areas of microanalyses.

**Table 3:** EDS microanalyses of the areas shown in Figure 3 in at. %.

	B	O	Al	Si	P	Ti	Cr	Mn	Fe	Ni	Cu	Zn	Mo	Pb
1	-	11.4	2.2	-	-	-	-	-	-	2.8	24.8	2.3	-	56.5
2	-	10.6	7.9	-	-	-	-	-	0.7	12.9	35.6	4.1	-	28.2
3	75.5	-	0.2	0.1	0.2	0.1	16.5	0.3	3.4	1.1	1.9	0.2	0.3	-
4	62.3	-	1.3	0.2	0.4	-	14.9	0.8	14.3	1.8	3.7	0.4	-	-
5	-	-	10.5	0.8	-	-	-	-	0.3	3.4	76.7	8.2	-	-
6	-	-	32.9	5.2	-	-	-	0.2	1.9	34.2	23.3	2.3	-	-

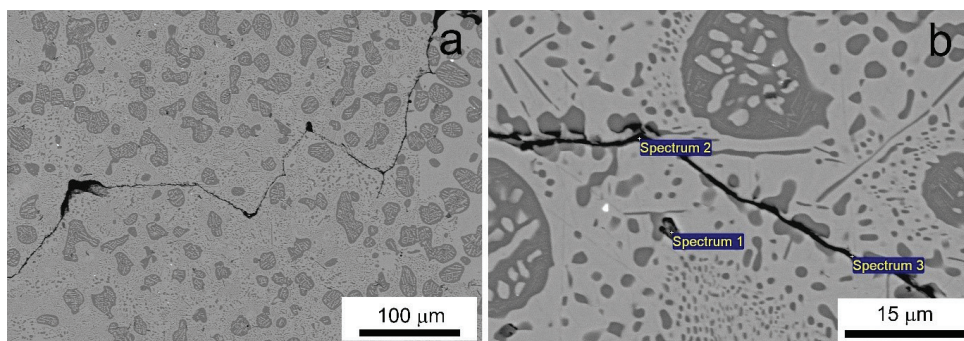


**Figure 4:** BE Images of the microstructure of a special copper alloy (a) and magnified detail with marked areas of microanalyses (b).

**Table 4:** EDS Microanalysis of the areas shown in Figure 4b in at. %.

	B	O	Mg	Al	Si	S	Cr	Mn	Fe	Ni	Cu	Zn	Pb	F
1	52.6			0.69			0.57	1.15	38.1	1.61	2.06			3.21
2		42.7	5.7	22.2		0.3			0.3	1.7	24.4	2.8		
3		35.5	4.3	19	0.7				0.5	11	24.9	3.9	0.3	

The particle in Region 1 represents the boride, which also contains iron, manganese, and chromium. Considering only boron, iron, manganese, and chromium, the composition of this boride is 56.9 at. % B, 41.2 at. % Fe, 1.2 at. % Mn, and 0.6 at. % Cr. Since this boride contains mainly only iron, we can primarily use the B-Fe binary system to look for a possible candidate. According to the binary system, only FeB exists with the space group Pbm $\bar{3}$  containing 50.0 at. % B. The other boride from the same binary system contains even less boron [8]. The borides from the ternary systems B-Cr-Fe and B-Fe-Mn [9, 14] all contain much smaller amounts of iron, so FeB, which also has infinite solubility of manganese and chromium, is the closest equilibrium phase. However, it is more likely that this boride is metastable and will continue to transform to a more stable form during cooling and service time.

Regions 2 and 3 correspond to a thin dark line, which, as shown by the analyses in Table 4, is aluminium oxide that also contains some magnesium. Other elements with significant contents are probably detected because of the low analytical spatial resolution. The formation of an aluminium-based oxide is to be expected since aluminium is the alloying element with the most thermodynamically stable oxides in this alloy and, consequently, all surfaces exposed to oxygen

would form this oxide. Such oxides are commonly found in these alloys.

Figure 5 shows light and BE images of the cast joint between the nickel insert and the special copper alloy and a dark thin line near the joint that resembles the oxides described earlier. Figure 5a shows part of a cast joint where mixing of both alloys took place. Such a joint is desirable. Figure 5b, on the other hand, shows an area of the joint where dark pores and a thin dark line are both present at the boundary between the special copper alloy and the nickel insert. It can be seen that no mixing took place in this part of the joint. Such areas are undesirable due to their inferior mechanical properties. In addition, these areas probably contain an oxide layer common in the investigated copper alloy, which by itself prevents the mixing of the two alloys. The shape of this oxide layer can also lead to the cracking and ultimate fracture of such a mould during service time. Figure 5c shows the BE image of a cast joint with a thin dark line near the joint similar to the aluminium-based oxides characterised earlier. In Figure 5d, this part is shown enlarged, and microanalyses were performed in two areas, as shown in Table 5. Both analyses confirm that aluminium-based oxides are present in both regions and probably contain some magnesium, chromium, and silicon. Other

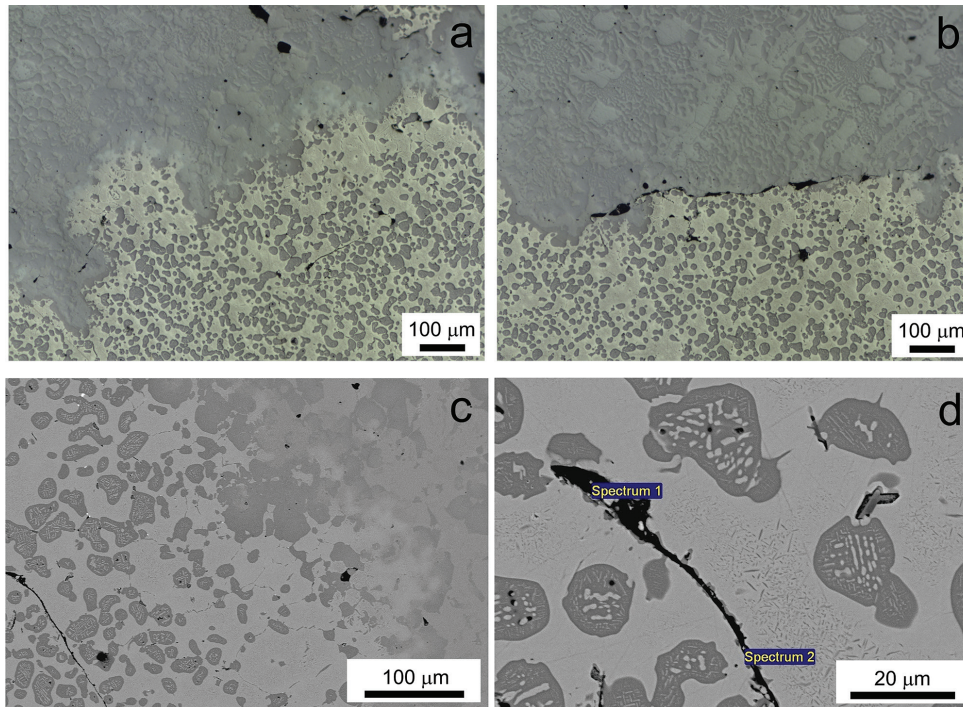


**Figure 5:** Light (a, b) and BE images (c, d) of the microstructure of a special copper alloy.

**Table 5:** EDS microanalysis of the areas shown in Figure 5d in at. %.

	O	Na	Mg	Al	Si	S	Ca	Cr	Mn	Fe	Ni	Cu	Zn
1	55.8	0.9	3.6	16.5	5.4	0.2	0.5	0.8	-	1.1	2.9	11.3	1.0
2	54.5	-	4.0	21.0	3.4	-	0.4	1.1	0.2	1.5	2.7	10.0	1.1

elements were most likely detected due to the low analytical spatial resolution.

The results of this work show that the special copper alloy contains several undesirable phases, many of which are a consequence of recycling. Lead and boride inclusions are certainly a result of recycling, while aluminium-based oxides found were probably formed during casting. However, aluminium-based oxides can also survive during remelting if not removed physically. These oxides could lead to the moulds cracking. Borides also accumulate in the alloy as a result of recycling. The borides found in this work are either iron-, iron-chromium-, or chromium-based, and all contain some manganese. These borides also have different morphologies and stoichiometries with respect to the metal/boron ratio and are not necessarily equilibrium phases. Some morphologies, such as the acicular morphology shown in Figure 3,

could also be potentially harmful, as they can lead to the formation of cracks.

## Conclusions

This work deals with the composition and microstructure of the nickel insert, the special copper alloy, and the cast joint between them.

The results show that the nickel insert contains 7 at. % Si and 0.3 at. % Fe. The special copper alloy, in addition to the intermetallic  $\beta$ -AlNi phase and the cubic copper-based solid solution, also contains some undesirable phases, including lead, aluminium-based oxides, and borides. Borides can be either iron-based, iron-chromium-based, or chromium-based with different stoichiometries for metallic components and boron. All of these borides also contain small amounts of manganese. Aluminium-based

oxides and some borides can potentially lead to cracking due to their morphology. The cast joint between the nickel insert and the special copper alloy generally shows mixing of the two alloys, which is desirable. In some areas of the joint, we observed porosity and, most likely, an oxide layer that prevented the two alloys from mixing. Such parts of the joint are not desirable, as they deteriorate the mechanical properties of the joint.

## Acknowledgements

The authors would like to acknowledge the financial support of the Slovenian Research Agency through the research programme P1-0195.

## References

- [1] Taylor, D.E., Black, W.T. (1992): Introduction to Copper and Copper Alloys. In: *ASM Handbook, Volume 2 – Properties and selection: Nonferrous Alloys and Special-Purpose Materials*, ASM International Handbook Committee (eds.). ASM International, Materials Park, Ohio, p. 228.
- [2] C99300 [online]. Copper Development Association Inc. [cited 23/08/2022]. Available on: <https://alloys.copper.org/alloy/C99300>.
- [3] C99350 [online]. Copper Development Association Inc. [cited 23/08/2022]. Available on: <https://alloys.copper.org/alloy/C99350>.
- [4] Wang, C.H., Chen, S.W., Chang, C.H., Wu, J.C. (2003): Phase Equilibria of the Ternary Al-Cu-Ni System and Interfacial Reactions of Related Systems at 800 °C. *Metallurgical and Materials Transactions A*, 34A, pp. 199–209.
- [5] Wang, W., Chen, H.L., Larsson, H., Mao, H. (2019): Thermodynamic constitution of the Al-Cu-Ni system modeled by CALPHAD and ab initio methodology for designing high entropy alloys. *Calphad*, 65, pp. 346–369, DOI:10.1016/j.calphad.2019.03.011.
- [6] Colín, J., Serna, S., Campillo, B., Rodríguez, R.A., Juárez-Islas, J. (2010): Effect of Cu additions over the lattice parameter and hardness of the NiAl intermetallic compound. *Journal of Alloys and Compounds*, 489, pp. 26–29, DOI:10.1016/j.jallcom.2009.09.034.
- [7] Liao, P.K., Spear, K.E. (1986): B-Cr. In: *ASM Handbook, Volume 3–Alloy Phase Diagrams*, ASM International Handbook Committee (eds.). ASM International, Materials Park, Ohio, p. 81.
- [8] Liao, P.K., Spear, K.E. (unpublished): B-Fe. In: *ASM Handbook, Volume 3–Alloy Phase Diagrams*, ASM International Handbook Committee (eds.). ASM International, Materials Park, Ohio, p. 81.
- [9] Homolová, V., Hiripová, L. (2017): Experimental Investigation of Isothermal Section of the B-Cr-Fe Phase Diagram at 1353K. *Advances in Materials Science and Engineering*, ID 2703986, pp. 1–7, DOI:10.1155/2017/2703986.
- [10] Nash, P., Nash, A. (1991): Ni-Si. In: *ASM Handbook, Volume 3–Alloy Phase Diagrams*, ASM International Handbook Committee (eds.). ASM International, Materials Park, Ohio, p. 318.
- [11] Baker, I., Yuan, J., Schulson, E.M. (1993): Formation of L1<sub>2</sub>-Structured Ni<sub>3</sub>Si. *Metallurgical and Materials Transactions A*, 24A, pp. 283–292.
- [12] Tokunaga, T., Nishio, K., Ohtani, H., Hasebe, M. (2003): Thermodynamic assessment of the Ni-Si system by incorporating ab initio energetic calculations into the CALPHAD approach. *Calphad*, 27, pp. 161–168, DOI:10.1016/S0364-5916(03)00049-X.
- [13] Zupanič, F., Bončina, T., Medved, J., Vončina, M. (2018): *Študija strjevanja nikelj-aluminijevega bronca 3 OMX z mikrostrukturno, EDS-mikrokemično, DTA, XRD analizo ter modeliranja s programom Thermocalc*. Fakulteta za strojništvo: Maribor, 26 p.
- [14] Repovský, P., Homolová, V., Čiripová, L., Kroupa, A., Zemanová, A. (2016): Experimental study and thermodynamic modelling of the B-Fe-Mn ternary system. *Calphad*, 55, pp. 252–259, DOI:10.1016/j.calphad.2016.10.002.
- [15] Liao, P.K., Spear, K.E. (1986): B-Mn. In: *ASM Handbook, Volume 3–Alloy Phase Diagrams*, ASM International Handbook Committee (eds.). ASM International, Materials Park, Ohio, p. 82.